A Mathematical Model for the Pessimum Size Effect of ASR in Concrete

A. Suwito[a], W. Jin[b], Y. Xi[a], C. Meyer[c]

[a] Dept. of Civil, Environmental, and Architectural Engineering, University of Colorado, Boulder, Colorado 80309
[b] Parsons Transportation Group/Steinman, New York, NY 10038
[c] Dept. of Civil Engineering and Engineering Mechanics, Columbia University, New York, NY 10027

ABSTRACT. This study proposes a mathematical model which characterizes the effects of various influential parameters on the pessimum size effect of ASR and predict the development of ASR expansion. The model emphasizes the chemomechanical coupling of the ASR expansion process, the size distribution of aggregates, and microstructural features of cement paste. The mechanical part of the model is developed based on a modified version of the generalized self-consistent theory. The chemical part of the model includes two opposing diffusion processes. One is the diffusion of chemical ions from pore solution into aggregate, and the other one is the permeation of ASR gel from the aggregate surface into the surrounding porous cement matrix. The total ASR gel is divided into two parts: the gel directly deposited in the interface pores which does not cause expansion, and the gel permeated into the surrounding pores in cement paste which generates the interface pressure and is responsible for the expansion. The amount of the first type of gel and the rate of the permeation of the second type of gel depends on the size of the aggregate and the porosity of the cement paste. The balance between the two opposing diffusion processes determines the pessimum size of the aggregate and maximum expansion of the concrete.

1. Introduction

Alkali-Silica reaction (ASR) in concrete is a reaction that involves the hydroxide ions in pore solution in cement paste and the reactive silica in aggregate. The main reaction product of ASR is called ASR gel and is located mainly in the interface zone between the aggregate and surrounding cement paste. In the presence of moisture, the ASR gel expands and generates significant interface pressure that may cause micro-cracks in concrete.

The mechanisms of ASR have been studied extensively. Research results for regular concrete showed that the maximum expansion due to ASR (referred to as pessimum expansion) depends on many parameters, such as the volume fraction, the type and size distribution of reactive aggregate, the composition and alkali content of the cement, the rate of strength development, and the mixture proportion of the concrete such as water-cement ratio (Diamond and Thaulow, 1974; Hobbs, 1988; Diamond, 1989; Johansen et al. 1993; Prezzi et al., 1997). Among the influential parameters, the size of aggregate plays an important role. The size of the aggregate that causes the pessimum expansion is called the pessimum size.

Several experimental methods have been developed for testing ASR behavior of concrete. Measuring directly the long-term expansion of concrete specimens has been considered to be the most reliable way to evaluate the reactivity of aggregate, but this is quite time consuming. Therefore, a number of accelerated test procedures have been devised that are now used with some confidence. Among the standard methods now available is the mortar bar test (ASTM C-227), the rock cylinder test (ASTM C-586), and the tests of ASTM C-289 and ASTM C-295. The most recently developed accelerated mortar bar test method is ASTM C-1260, which requires only 14 days of testing. The performances of some of the standard test methods were compared by Alasali et al. (1991).

Parallel to the extensive efforts to establish standard testing methods, much attention has also been paid to the development of theoretical models for characterizing ASR behavior. Groves and Zhang (1990) developed a dilatation theory based on the observation of the microstructure of an expanded mortar composed of silica glass particles in ordinary Portland cement paste. In the dilatation model, it was assumed that the main ASR product is formed on the surface of silica glass particles. The formed gel causes a dilatation of the matrix. The overall expansion of the mortar was obtained using the elasticity theory of a misfitting sphere in the matrix.

The dilatation model was combined with various diffusion theories to characterize ASR-induced expansion (Svensson 1991; Furusawa et al., 1994; and Goltermann 1994). The expansion process of the concrete is divided into two stages: (1) the diffusion of the hydroxide and alkali ions into aggregate, followed by the reaction of these ions with the reactive silica in the aggregate; and (2) the development of the ASR induced expansion, which is similar to the dilatation theory. In the second stage of the expansion process, Furusawa et al. (1994) further assumed that there exists a porous zone around the aggregates and that the expansion is initiated only when the volume of the reaction products exceeds the available volume of the porous zone.

A fracture mechanics theory was recently developed by Bazant et al. (2000), in which the stress intensity factor at the preexisting flaws near the surface of the reactive particles is used to evaluate the crack propagation due to the pressure generated by the ASR gel. Ulm et al. (2000) established a detailed model of ASR kinetics and included ASR heat diffusion and analyzed the effect of ASR on different sizes of structures.

The purpose of the present paper is to develop a theoretical model for predicting the pessimum expansion of concrete and the pessimum size of aggregate. The significance of the pessimum size in engineering practice has been pointed out in recent experimental studies at Columbia University, New York, by Meyer and Baxter (1998), Jin (1998), and Meyer and Xi (1999). Using waste glass particles of various sizes in concrete and the accelerated mortar bar test (ASTM C-1260), they demonstrated that a decrease of particle size causes an increase of volume expansion and damage due to ASR up to a specific particle size (pessimum). However, when the particle size is reduced further, smaller ASR induced expansions were observed, together with an increase in compressive strength of the concrete. This result is significant particularly if highly reactive aggregate such as crushed waste glass is used. Basically, if such aggregate is crushed to a size smaller than the pessimum value, then, instead of causing the deleterious expansion in concrete, the problem of ASR can be controlled.

Relatively little research effort has focussed on predicting the pessimum expansion of concrete and the pessimum size of aggregate. The basic idea and a brief outline of the present model were presented in two recent conferences (Jin et al. 1998; Xi et al. 1999), however, the main part of the model and its numerical implementation have been completed only recently. Another recent paper on this topic was published by Bazant and Steffen (2000), in which the ASR kinetics was characterized in detail and the pessimum size of aggregate given in terms of the effect of internal pore relative humidity on ASR expansion.

The present theoretical model is divided into two parts. The first part is the application of a composite theory to characterize the expansion and internal pressure generated by ASR with reactive aggregate of different sizes. The second part is the application of diffusion theories to simulate the dominant diffusion processes during ASR in concrete. The pessimum size of aggregate is obtained by combining the composite and diffusion models with the micro-structural features of concrete such as cement paste porosity and aggregate gradation. The composite model in the first part is general and can be used for various situations, while the diffusion related model in the second part is developed particularly for simulating the testing environment of ASTM C-1260.

2. The Composite Model for ASR Expansion

In general, the expansion caused by ASR can be simulated by the thermal expansion of an inclusion in a composite. Thus, the total expansive strain of concrete can be determined using the models developed for effective thermal expansion of composites. In this study, the model used to evaluate the effective ASR-induced expansion of concrete is based on the multiphase generalized self-consistent method developed by Xi and Jennings (1997), in which the basic material element is a composite spherical system with one constituent phase associated with another. The center sphere is the aggregate and the outside layer is the cement paste matrix as shown in Fig. 1.

2.1 Configuration of the Microstructure

For two-phase composite materials, the typical configuration of microstructure is shown in Fig. 2. The structure of the material can be divided into many regions or elements such that the volume fraction of each phase in each region (or element) is the same. The partition may be made so that the elements approach the spherical surfaces. Therefore, Fig. 2 is assumed to be equivalent to Fig. 3. In theory, the shape of the element could vary, for example cubic, but spherical elements have the advantage of being three-dimensional, while at the same time reducing the problem to one dimension. The basic element of the microstructure in Fig. 3 is then a composite sphere composed of two different phases in which the ratio of radii R_1/R_2 is a constant. As a result of the constant volume fraction, the basic element is independent of the absolute size of the spheres. For the material under consideration, i.e. concrete, phase 1 is the aggregate and phase 2 is the matrix.

The configuration of the basic element shown in Fig. 3 can also be used to model heterogeneous multiphase composite materials, which means that there could be multiple layers outside of the center sphere. The total number of phases in a composite depends on the composite material to be characterized. For the problem of ASR-induced expansion, we decided to use the two-phase composite model with the ASR gel included as part of the aggregate. The ASR gel is not considered a distinct phase mainly because each phase is assumed to have a fixed volume fraction in each basic element (the ratio of radii R_1/R_2 is a constant). The thickness of the gel layer formed at the aggregate surface at a certain time is constant and not proportional to the size of aggregate. This means, if we were to consider the gel as a distinct phase, we would have different volume fractions of the gel phase for different sizes of aggregate.

The configuration of the system in Fig. 3 requires a specific gradation of element sizes such that each composite sphere has the same internal structure, while the smaller elements fill the gaps between adjacent spheres. Obviously, such a particle size distribution requires a broad range of particle sizes. The aggregates used in concrete have such a broad range of size distribution, from the micrometer to the centimeter. The size of typical fine aggregate (i.e. sand) ranges from 100 micrometer (and less) to 4.75 mm, and the size of coarse aggregate (i.e. gravel) ranges from 4.75 mm to several centimeters (or larger).

Considering the micro-structural configuration shown in Fig. 3, one can equivalently obtain Fig. 4, where the phase 3 is the effective homogenous medium equivalent to the heterogeneous medium in Fig. 2.

2.2 ASR-induced Expansion of Concrete with Different Aggregate Sizes

The three-phase model shown in Fig. 3 was used by Christensen (1979) and Christensen and Lo (1979) to determine the effective elastic properties of two-phase composites, such as bulk modulus and shear modulus. Based on this idea, Xi and Jennings (1997) used the generalized self-consistent method to determine the effective shrinkage in homogenous media. To model ASR-induced expansion due to aggregates with different sizes, we will modify the effective shrinkage model and derive the effective expansion coefficient for the two-phase composite. The interface pressure between the aggregate and cement paste matrix, which plays an important role in the expansion process of ASR, will also be derived.

Applying elasticity theory to the element of Fig. 4, for any single phase that expands, say phase i, the equilibrium equation in spherical coordinates is

$$U_{i,rr} + \tfrac{2}{r}U_{i,r} - \tfrac{2}{r^2}U_i - \frac{1+\nu_i}{1-\nu_i}\alpha_{i,r} = 0 \qquad (1)$$

where U_i is the displacement of the phase i in the radial direction; r is the radial location coordinate; $U_{i,r}$ and $U_{i,rr}$ are the first and second derivative of U_i with respect to r; and ν_i and α_i are Poisson's ratio and linear expansion of phase i, respectively. Since the expansion due to ASR in the linear elastic range is very small, the term associated with the differential linear expansion, $\alpha_{i,r}$, can be neglected. Thus Eq. (1) can be simplified as

$$U_{i,rr} + \tfrac{2}{r}U_{i,r} - \tfrac{2}{r^2}U_i = 0 \qquad (2)$$

Eq. (2) is the basic differential equation that applies to any phase shown in Fig. 4. When all phases expand, but each with its own coefficient of expansion, the solution of Eq. (2) is

$$U_i = C_i r + \frac{D_i}{r^2} \qquad \sigma = 3K_iC_i - 4G_i\frac{D_i}{r^3} - 3K_i\alpha_i \qquad (3)$$

where σ_i is the stress of phase i in the radial direction; K_i and G_i are the bulk modulus and shear modulus of phase i, respectively; and C_i and D_i are constants, with $D_i = 0$ to avoid the singularity at $r = 0$.

Eq. (3) is the general solution and valid for all phases, only the integration constants C_i and D_i are different for each phase and can be determined using continuity conditions at $r = R_1$ and the boundary condition at $r = R_2$. The continuity conditions at $r = R_1$ are

$$U_1(R_1) = U_2(R_1) \qquad \sigma_1(R_1) = \sigma_2(R_2) \tag{4}$$

and the boundary condition at *r* = *R₂* is

$$U_2(R_2) = \delta \tag{5}$$

in which δ is a radial displacement due to the expansion of the element at $r = R_2$. Applying the continuity conditions of Eq. (4) to Eq. (3) we have

$$C_1 R_1 = C_2 R_1 + \frac{D_2}{R_1^2} \tag{6}$$

and

$$3K_1 C_1 - 3K_1 \alpha_1 = 3K_2 C_2 - 4G_2 \frac{D_2}{R_1^3} - 3K_2 \alpha_2 \tag{7}$$

Imposing the boundary condition, Eq. (5), on Eq. (3) gives

$$U_2(r = R_2) = C_2 R_2 + \frac{D_2}{R_2^2} = \delta \tag{8}$$

The three constants C_1, C_2, and D_2 can be solved using Eqs. (6), (7), and (8) in terms of the displacement δ.

To determine an effective expansion coefficient, α_{eff}, we need to consider the continuity condition at $r = R_2$, for the composite sphere and an effective homogenous sphere of the same volume, in which the displacement and the stress should be the same as in the composite sphere. The displacement continuity leads to

$$U_{eff}(r = R_2) = C_{eff} R_2 = \delta \qquad \Rightarrow C_{eff} = \frac{\delta}{R_2} \tag{9}$$

and the stress continuity to

$$3K_{eff}\frac{\delta}{R_2} - 3K_{eff}\alpha_{eff} = 3K_2C_2 - 4G_2\frac{D_2}{R_2^3} - 3K_2\alpha_2 \tag{10}$$

where the subscript “eff” stands for effective homogenous medium. Substituting C$_2$ and D$_2$ into Eq. (10) and taking α_1, α_2, and α_{eff} as zero, we can determine the effective bulk modulus K_{eff} as

$$K_{eff} = \frac{K_2(3K_1 + 4G_2) - 4V_1G_2(K_2 - K_1)}{(3K_1 + 4G_2) + (3K_2 + - 3K_1)V_1} \tag{11}$$

in which $V_1 = R_1^3 / R_2^3$, the volume fraction of the phase 1. By substituting Eq. (11) into Eq. (10), the effective expansion coefficient for homogenous media is obtained

$$\alpha_{eff} = \frac{K_1\alpha_1V_1(3K_2+4G_2) + K_2\alpha_2(1-V_1)(4G_2+3K_1)}{K_2(3K_1+4G_2) - 4V_1G_2(K_2-K_1)} \tag{12}$$

In the case of concrete, the aggregate is the constituent phase that expands during ASR, and the cement paste matrix does not expand. Therefore, Eq. (12) can be simplified by taking α_2 as zero, that is

$$\alpha_{eff} = \frac{K_1V_1(3K_2+4G_2)}{K_2(3K_1+4G_2) - 4V_1G_2(K_2-K_1)}\alpha_1 \tag{13}$$

The final step in the derivation is to find an expression for the interface pressure, P_{int}, between the aggregate and the matrix. By using the stress equation, Eq. (3), the interface pressure is obtained as

$$P_{\text{int}} = -\sigma(R_1) = \frac{12K_1K_2G_2(1-V_1)}{4V_1G_1(K_1-K_2) + K_2(3K_1+4G_2)}\alpha_1 \tag{14}$$

It should be noted that the composite model used in the present study assumes that the concrete and all its constituents can be treated as elastic materials. This means that the model of ASR-induced expansion developed in this paper is applicable only for predicting concrete behavior with initial and moderate expansion due to ASR. For situations that lead to severe map cracking, more sophisticated models need to be developed to account for the damage due to inelastic and fracture behavior of the cement paste around each individual aggregate.

The unknown parameter in Eq. (13) is the expansion coefficient of aggregate due to ASR, α_1. In contrast to the thermal expansion of conventional composites, the ASR induced expansion of aggregate is size dependent. In other words, two aggregate particles of the same mineralogical makeup but with different sizes expand differently. This is why ASR causes the special phenomenon known as the pessimum expansion. As a result, the overall ASR expansion of the concrete must be determined not simply by Eq. (13), but as the volumetric average of ASR expansions of the basic elements with different sizes.

$$\alpha_{eff} = \sum \phi_i \alpha_{eff}^{Ri} \tag{15}$$

in which ϕ_i is the volume fraction of aggregate with size R_i and α_{eff}^{Ri} the ASR expansion of the basic element of concrete with the size of aggregate, R_i. It is important to note that the volume fraction V_1 in Eq. (13) is different from ϕ_i in Eq. (15). V_1 is the volume fraction of the total amount of aggregate based on the total volume of concrete. ϕ_i is the volume fraction of the aggregate of size R_i based on the total amount of aggregate and is given by the aggregate grading curve.

3. Mechanisms for Pessimum Effect of ASTM C-1260 Specimens

In the ASTM C-1260 test, a mortar bar (2.54 cm by 2.54 cm by 25.4 cm) is made with a specified water-cement ratio, aggregate volume and five different aggregate sizes. The mortar bars are moisture cured for one day prior to demolding and then immersed in a sodium-hydroxide solution for 14 days. The short curing period of one day is to ensure that no significant ASR occurs before the test, and that the pore relative humidity does not drop significantly due to the hydration reaction. During the testing period, the samples are taken out of the solution daily for measuring the length change, which takes only a few minutes. Therefore, the internal pores of the specimens are almost always fully saturated, and the moisture diffusion is insignificant. In fact, the test was designed this way so that there is enough supply of water for the expansion of ASR gel to occur at an accelerated rate. The test is further accelerated by the solution's elevated temperature of 80°C and high alkali concentration (1 N NaOH).

Two transport processes govern the behavior of specimens during the ASTM C-1260 test. First, there is the penetration of alkali ions into the specimen, which can be further divided as the penetration of the ions from the specimen boundary into the specimen, called macro-diffusion, and the penetration from the surface of each aggregate particle into the aggregate, called micro-diffusion. Once the concentration of alkalis within a reactive aggregate reaches a certain level, ASR gel forms. Because of the porous interface zone surrounding the aggregate, the ASR gel formed during the initial stage deposits directly inside the interfacial pores, and thus, there is no expansion of the concrete. When the volume of the gel exceeds the capacity of the interfacial pores, an interface pressure is generated and the second transport process takes place, which is the permeation of the ASR gel into the pores of the cement paste and which is responsible for the expansion. The total ASR gel can thus be divided into two parts, one that is deposited directly in the interfacial pores, and one which permeates into the surrounding cement paste.

Apparently, the ASR expansion of ASTM C-1260 specimens is a combined result of these two opposing transport processes. Depending on which process dominates, there are two possible outcomes. If the volume of ASR gel formed is much larger than the volume of the interface porous zone, the gel pressure builds up and causes severe expansion. This is the case dominated by the diffusion of alkali ions and the reaction of alkali and silica and is defined as the reaction dominant case. On the other hand, if the interfacial porous space is sufficient to accommodate all ASR gel, then there is only minor or no expansion. This is the case dominated by the permeation of ASR gel and is defined as the permeation dominant case.

To study the pessimum effect of ASR, let us consider aggregate particles with size R. The amount of ASR gel formed at a certain time during the test depends on the total volume and surface area of the aggregate. For a fixed aggregate volume, the surface area is a function of the size R. The smaller R is, the larger the surface area, and the higher the rate of ASR. Therefore, as a general rule, a decrease of R should result in an increase of ASR expansion if only the reaction dominant case were considered, as characterized by the ascending curve of Fig. 6. Reducing the size R below a certain size (the pessimum size) leads to the permeation dominant case. Here the aggregate particles are small enough that the amount of the gel formed around each particle is comparable to the pore space available in the surrounding cement paste. Therefore, the gel pressure is released and the ASR expansion reduced. Since the porosity of cement paste is independent of aggregate size, any further decrease of R reduces the amount of ASR gel formed around each particle and thus reduces the ASR expansion. This is characterized in Fig. 6 by the descending branch of the curve. In the limiting case that R is so small that the interfacial pore space can hold all ASR gel even if the entire aggregate particle turns into gel, there will be no ASR expansion at all. The peak separating the ascending and descending curve branches in Fig. 6 corresponds to the pessimum aggregate size.

The above analysis explains why the pessimum size depends on the pore space in the interfacial zone and the porosity of cement paste. The higher the porosity, the larger the pessimum size. This general conclusion has been verified experimentally by using an air-entraining agent to increase the concrete porosity (Jin 1998). Larger dosages of air-entraining agent generate more air bubbles in the cement paste as well as in the interface zone, thereby increasing the pessimum size of the aggregate.

Below, a mathematical description of this basic mechanism shall be outlined. It should be pointed out that it applies only to the special case in which the concrete is fully saturated. It does not describe the ASR process in realistic situations, in which the pore structure of the concrete is partially saturated and thus moisture diffusion must be taken into consideration in addition to the other two governing transport processes, namely alkali ion diffusion and ASR gel permeation. The effect of moisture diffusion on pessimum size was analyzed in detail by Bazant and Steffens (2000).

4. Mathematical Model for Diffusion of Alkali Ions

As described above, alkali ions penetrate from the specimen boundary into the concrete (macro-diffusion), and then into the aggregate (micro-diffusion). The macro-diffusion of alkali ions is similar to other macro-diffusion processes in concrete (such as moisture diffusion and chloride penetration), which have been studied extensively (Xi et al., 1995a, 1995b; Xi and Bazant 1999). In the present study, we focus on the process of micro-diffusion, which may be described by Fick's law

$$B_{ion}\frac{\partial C_{ion}}{\partial t}=\nabla\left(D_{ion}\nabla C_{ion}\right) \tag{16}$$

in which C_{ion} is the free ion concentration of the pore solution inside the aggregate, which could be hydroxide ions, calcium ions, sodium ions, etc. B_{ion} and D_{ion} are the binding capacity and ion permeability of the aggregate, respectively. B_{ion} and D_{ion} may not be simple constants but depend on the microstructure of the aggregate as well as the type of ions under consideration. After a layer of ASR gel has formed on the aggregate surface, B_{ion} and D_{ion} represent not only the binding capacity and the permeability of the aggregate but also of the ASR gel, because the alkali ions must penetrate the ASR gel first and then diffuse into the aggregate.

When the angularity of aggregate is low (round shaped aggregate such as river sand), the aggregate may be simulated as a sphere, and the diffusion equation may be formulated in a polar coordinate system and solved analytically. The initial condition is C_{ion} = 0 for t = 0 in the aggregate. The boundary condition on the aggregate surface is C_b = C_0 (a constant ion concentration), and the boundary condition at the center of the aggregate particle is C_{ion} = 0. The solution of Eq. (16) in a polar coordinates is

$$C_{ion}(r,t)=C_0+\frac{2R_iC_0}{\pi r}\sum_{n=1}^{\infty}\frac{(-1)^n}{n}\exp\left(\frac{-\kappa n^2\pi^2 t}{R_i^2}\right)\sin\frac{n\pi r}{R_i} \tag{17}$$

in which $\kappa = D_{ion} / B_{ion}$.

It should be pointed out that at the initial stage of the mortar bar test, not all aggregate particles have the same boundary condition C_b, because the alkali ions penetrate from the boundary into the mortar bar. So, for a particle located at a certain distance from that boundary, the boundary condition is not constant but a function of time. With a time dependent boundary condition, $C_b = C_0(t)$, Eq. (16) can still be solved analytically, but the solution will not be given here. $C_0(t)$ can be obtained from macroscopic diffusion analysis of the mortar bar. Here, we assume that the macro-diffusion affects the boundary conditions of some aggregate particles only during the initial stage. Because of the small mortar bar size (1.27 cm from the surface to the center of the bar), the macro-diffusion reaches equilibrium very soon and the boundary condition for all aggregates equals the concentration of the solution, which is constant.

The ASR process takes place within the surface layer of each aggregate particle, where C_{ion} reaches a certain concentration level. Eq. (17) can be solved inversely to determine the thickness of the ASR layer, r. The volume of the reacted portion of the aggregate particle of size R_i, V_{Ri}, can then be calculated

$$V_{Ri} = \left[\frac{R_i^3 - (R_i - r)^3}{R_i^3}\right]\left(\frac{4}{3}\pi R_i^3\right) = \left[1 - \left(1 - \frac{r}{R_i}\right)^3\right]\left(\frac{4}{3}\pi R_i^3\right) \tag{18}$$

This volume can be converted into the volume of ASR gel, V_{gel}^{Ri}, which is

$$V_{gel}^{Ri} = \eta V_{Ri} \tag{19}$$

where η is the volume ratio of the ASR gel to the reacted aggregate. Apparently, η must be greater than 1 for ASR expansion to occur. η can be determined approximately from the reaction kinetics of ASR (Groves and Zhang, 1990; Furusawa et al., 1994).

5. Mathematical Model for Permeation of ASR Gel

It was observed that there exists a porous zone between the aggregate and the surrounding cement paste matrix (Ping et al. 1991; Bentz and Garboczi 1991). The ASR gel formed at the outside of the aggregate fills this porous zone immediately and once it has filled it completely, it starts to generate interfacial pressure, which pushes the gel to further permeate the pore structure of the cement paste. Mathematically, this process can be described as

$$V_{gel,eff}^{Ri} = V_{gel}^{Ri} - V_{pore}^{Ri} \tag{20}$$

where $V_{gel,eff}^{Ri}$ is the effective volume of the gel generating the interfacial pressure and further permeating into the porous cement paste; V_{gel}^{Ri} is the total volume of the gel formed by aggregate particles of size R_i (Eq. 19); V_{pore}^{Ri} is the total volume of pores in the surrounding interface zone. V_{pore}^{Ri} can be calculated using

$$V_{pore}^{Ri} = V_{unit} A_{agg}^{Ri} \tag{21}$$

where V_{unit} is a material constant (a length scale) representing the capacity of the porous zone to absorb ASR gel per unit area, and A_{agg}^{Ri} is the surface area of an aggregate particle of size R_i.

In the process described above, a part of the ASR gel directly deposits within V_{pore}^{Ri}, and there is no diffusion analysis needed. If ASR gel permeates through porous cement paste, a diffusion analysis must be conducted, which can be characterized by Darcy's law for a viscous flow as

$$\frac{\partial C_{gel}}{\partial t} = \nabla\left(\frac{\kappa_{gel}}{\eta_{gel}} \nabla P_{gel}\right) \tag{22}$$

in which C_{gel} and η_{gel} are the concentration and viscosity of the gel, respectively; κ_{gel} is the gel permeability of the porous cement paste; and P_{gel} is the pressure distribution in the gel, which depends on the degree of saturation of the pores. At the boundary, the interface pressure, P_{int}, is applied.

The stress distribution, P_{gel}, may be determined by solving the boundary value problem for a thick-walled sphere with an internal pressure P_{int} applied on the internal boundary. Then, the concentration profile of the ASR gel may be determined by solving the permeation equation with a state equation. However, the interfacial pressure P_{int} is unknown and a function of time and needs to be evaluated simultaneously from the equilibrium of the composite system, the diffusion of ions, and the permeation of the gel. One can see that this is a chemo-mechanical coupled problem (Jin, 1998).

In order to solve the coupled equations, a state equation must be introduced, which relates the concentration of ASR gel in the pores, C_{gel}, the gel pressure P_{gel}, and the temperature, T.

Unfortunately, there has been a lack of experimental data and theoretical models for the state equation of ASR gel in porous cement paste matrix. As a first approximation, a simplified state equation can be developed by taking the temperature as a constant (T = 80 °C in ASTM C-1260), so, the state equation may be written as

$$C_{gel} = \beta P_{gel} \tag{23}$$

in which β is the state function for cement paste, which may be determined by the state of saturation. When the pores in the cement paste are saturated with ASR gel, $C_{gel} = C_p$, where C_p is the porosity of the cement paste. At the same time, the pressure P_{gel} reaches the saturation pressure, which can be taken approximately as the tensile strength of the cement paste, f_t'. Therefore, $\beta = C_p/f_t'$. With the state equation Eq. (23), the permeation equation, Eq. (22), can be expressed in terms of C_{gel} (or P_{gel}). The initial condition is $C_{gel}(r,0) = 0$. The boundary condition at the interface is $C_{gel}(R_i,t) = \beta P_{int}(t)$; and the boundary condition at the far field is $C_{gel}(R_{if},t) = 0$; where R_{if} is the far field distance of the aggregate with size R_i, which can be taken as half the average spacing between two aggregate particles. Eq. (22) with the boundary and initial conditions can then be solved analytically

$$\begin{aligned} C_{gel}(r,t) = {} & \frac{2\beta}{r\left(R_{if} - R_i\right)} \sum_{n=1}^{\infty} \exp\left[\frac{-\nu n^2 \pi^2 t}{\left(R_i - R_{if}\right)^2}\right] \sin\left[\frac{n\pi\left(r - R_i\right)}{\left(R_{if} - R_i\right)}\right] \\ & \left\{\frac{-n\nu\pi R_i}{\left(R_i - R_{if}\right)} \int_0^t \exp\left[\frac{\nu n^2 \pi^2 \lambda}{\left(R_i - R_{if}\right)^2}\right] P_{\text{int}}(\lambda) d\lambda\right\} \end{aligned} \tag{24}$$

in which $\nu = \kappa_{gel} / \eta_{gel}$. Eq. (24) is used as the solution of the permeation equation for each size R_i of the aggregate.

Eq. (24) is not a closed-form solution because $P_{int}(t)$ as the boundary condition at the interface is unknown and must be solved together with the coupled mechanics problem. A piecewise time step numerical procedure was developed to solve the chemo-mechanically coupled problem as described in the next section.

The gel volume in the porous cement paste surrounding an aggregate particle with size R_i at time t, V_{pg}^{Ri} may be evaluated by integrating the gel concentration over the surrounding cement paste,

$$V_{pg}^{Ri} = \int_{R_i}^{R_{if}} 4\pi r^2 C_{gel}\, dr \tag{25}$$

The volume change due to ASR of aggregate with size R_i is $\Delta V_{gel}^{Ri} = V_{gel,eff}^{Ri} - V_{pg}^{Ri}$. It should be emphasized that ΔV_{gel}^{Ri} is not the increment of the total ASR gel, but the volume of the ASR gel beyond the accommodating capacity of interfacial pores, V_{pore}^{Ri}, and the pores in the bulk cement paste. By assuming the isotropic behavior for concrete, the coefficient of expansion for the aggregate with size R_i due to ASR is

$$\alpha_1^{Ri} = \frac{\Delta V_{gel}^{Ri}}{V_a^{Ri}} = \frac{V_{gel,eff}^{Ri} - V_{pg}^{Ri}}{V_a^{Ri}} = \frac{V_{gel}^{Ri} - V_{pore}^{Ri} - V_{pg}^{Ri}}{V_a^{Ri}} \tag{26}$$

The volume change ΔV_{gel}^{Ri} at a certain time generates a pressure $P_{int}(t)$ between the aggregate and the matrix. With the given ΔV_{gel}^{Ri}, $P_{int}(t)$ can also be solved from the equilibrium of the composite system. The $P_{int}(t)$ thus solved must be equal to the $P_{int}(t)$ in the state equation, which was used to solve Eq. (22).

6. Numerical Procedure

Equations (13, 14, 15, 19, 20, 24 and 25) form a complete model for ASR expansion. It is impossible to solve the problem analytically because the diffusion and the permeation of the gel are coupled with the interface pressure. Instead, a detailed numerical procedure shall be presented.

An important detail of the solution procedure is how to handle Eq. (24), in which the interface pressure, $P_{int}(t)$, appears inside the integral. This interface pressure is assumed to vary linearly within each time step. This assumption does not lead to a significant loss of accuracy provided that the time steps are small enough. Using this approach, the analytical solution of Eq. (24) can be used to determine the gel distribution in the porous zone of the cement paste.

The step by step procedure employed in the numerical analysis is as follows:

1. Provide input data for the analysis, such as the number of different aggregate sizes, the different sizes and volume fractions, etc.
2. For the aggregate of size R_i, conduct the piecewise time step integration through the time domain of specified duration.
3. Calculate the depth of ion penetration into the aggregate, r.
4. Compute the ASR gel layer formed at the surface of the aggregate adjusted for the presence of pores in the interface zone.
5. Assume an interface pressure, P_{int}.
6. Compute the gel permeation distribution and calculate the volume of gel which permeates into the matrix.
7. Calculate the volume change of gel, ΔV_{gel}^{Ri}, and the expansion of the aggregate, α_1^{Ri}.
8. Calculate the interface pressure using the model of composite mechanics, Eq. (14).
9. Compare the two interface pressures obtained in step (8) and (5). If their difference is within the prescribed tolerance level, continue to the next step, otherwise go back to step (5) and iterate until the convergence criterion is satisfied.
10. Calculate the expansion coefficient of ASR for the aggregate of size R_i.
11. Repeat steps (2) to (10), calculating expansion coefficients for all aggregate sizes, then determine the overall coefficient of expansion of concrete as the volumetric average of Eq. (15).

7. Numerical Results

There are many material parameters involved in the two transport models and the composite model which need to be determined to reflect the physical, chemical, and micro-structural features of both cement paste and aggregate. Table 2 lists the material parameters used to obtain the numerical results of the model presented in Figures 7-11. Fig. 7 shows the ion concentration profile in an aggregate particle of size 0.6 mm. The concentration profile of ASR gel in the pores of the cement paste surrounding the aggregate is given in Fig. 8. The coordinate for the radius starts at 0.6 mm, which is the surface of the aggregate. Fig. 9 shows the development of the interface pressure build-up with time up to 14 days, simulating the ASTM C-1260 test. As one can see, the interfacial pressure is sufficiently high to cause fracture of the material. The fact that in many tests the specimens do not crack can be explained with any one of the important factors that were disregarded here, such as the release of the stress concentration by micro-cracking and by the high creep of the cement paste at early ages (only 14 days old). Moreover, the strength of the cement paste in small specimens is much higher than in large concrete members, because of the reduced probability of defects (Grooves and Zhang 1990).

The curve identified in Fig. 10 as "Xi" shows the increase of ASR expansion with time, in which Eq. (12) and Eq. (15) are used to evaluate the coefficient of expansion. The curve marked as "Hashin" represents Hashin's bound (Hashin 1962; Christensen 1979), which was used together with Eq. (15) to calculate the coefficient of expansion. One can see that the results of the two models agree very well.

Fig. 11 compares the numerical ASR expansions for different aggregate sizes with the experimental results obtained by Jin (1998). For the material parameters listed in Table 2, it is evident that the pessimum size of the aggregate is #200, which is about 0.075 mm. This pessimum size agrees with the one obtained by Jin (1998) and Meyer and Baxter (1998).

8. Summary and Conclusions

1. A mathematical model was developed which characterizes the effects of various influential parameters on the pessimum effect of ASR and can predict ASR expansion. The model encompasses the chemo-mechanical coupling of the ASR expansion process, the size distribution of aggregates, and micro-structural features of the cement paste.
2. The mechanical part of the model is developed based on a modified version of the generalized self-consistent theory. The chemical part of the model includes two opposing diffusion processes. One is the diffusion of chemical ions from pore solution into aggregate,

and the other one is the permeation of ASR gel from the surface of aggregate out to the surrounding porous cement paste matrix.

3. The total ASR gel formed is divided into two parts: the gel directly deposited in the interface pores which is not governed by diffusion and does not cause expansion; and the gel permeated into the surrounding pores in cement paste which generates interface pressure and is responsible for the expansion. The amount of the first type of gel and the rate of the permeation of the second type of gel depend on the aggregate size and the porosity of the cement paste.
4. For a fixed volume of aggregate, a decrease of aggregate size results in an increase of ASR expansion (due to increased surface area), which is the diffusion dominant process. When the aggregates are small enough that the amount of ASR gel formed around each aggregate is comparable to the pore space available in the surrounding cement paste, the gel pressure is released and the ASR expansion is reduced, which is the permeation dominant process. In the limiting case that the aggregate size is so small that the interfacial pore space can hold all ASR gel even if the entire aggregate turns into the gel, there will be no ASR expansion at all. The size for which the two diffusion processes are balanced is the pessimum aggregate size.
5. The pessimum size depends on the pore space in the interfacial zone and the cement paste porosity. The higher the porosity the larger the pessimum size.
6. The model presented here is capable of simulating the development of ASR expansion and predicting the pessimum size of reactive aggregates. The model provides a general framework, and further research is needed for experimentally determining the various material parameters and to validate the model with more test data.

9. Acknowledgement

Partial financial support under NSF grant CMS-9872379 to University of Colorado at Boulder is gratefully acknowledged. Also, partial financial support under Colorado DOT grant OE HAA 98HQR000088 to University of Colorado at Boulder is gratefully acknowledged.

10. References

Alasali, M.M., Malhotra, V.M., and Soles, J.A. (1991) "Performance of Various Test Methods for Assessing the Potential Alkali Reactivity of Some Canadian Aggregates", ACI Materials Journal, Nov. -Dec., 88(6), 613-619.

Bazant, Z.P., and Steffens, A., (2000) "Mathematical Model for Kinetics of Alkali-Silica Reaction in Concrete", *Cement and Concrete Research*, 30, 419-428.

Bazant, Z.P., Zi, G., and Meyer, C., (2000) "Fracture Mechanics of ASR in Concretes with Waste Glass Particles of Different Sizes", *J. of Engineering Mechanics*, ASCE, 126(3), 226-232.

Bentz, D.P. and Garboczi, E.J., (1991) "Simulation Studies on the Effects of Mineral Admixtures on the Cement Paste Aggregate Interfacial Zone", *ACI Material Journal*, Sept.-Oct., 518-529.

Christensen, R.M., (1979) "*Mechanics of Composite Materials*," Wiley-Interscience, New York.

Christensen, R.M., and Lo, K.H., (1979) "Solutions for Effective Shear Properties in Three Phase Sphere and Cylinder Models," *J. Mech. Phys. Solids*, 27, 315-330.

Diamond, S. (1989) "ASR-Another Look at Mechanisms", *Alkali-Aggregate Reaction*, Proc. of the 8th Int. Conf., Kyoto, Japan, Elsevier Applied Science, 83-94.

Diamond, S. and Thaulow, N. (1974) "A Study of Expansion due to Alkali-Silica Reaction as Conditioned by the Grain Size of the Reactive Aggregate", *Cement and Concrete Research*, 4, 591-607.

Furusawa, Y., Ohga, H., and Uomoto, T. (1994) "An Analytical Study Concerning Prediction of Concrete Expansion Due to Alkali-Silica Reaction", *Proc. of 3rd Int. Conf. on Durability of Concrete*, Nice, France, Editor Malhotra, SP 145-40, 757-780.

Goltermann, P. (1994) "Mechanical Predictions on Concrete Deterioration. Part 1: Eigenstresses in Concrete", *ACI Materials Journal*, Nov., and Dec., 91(6), 543-550.

Groves, G.W., and Zhang, X. (1990) "A Dilatation Model for the Expansion of Silica Glass/OPC Mortars", *Cement and Concrete Research*, 20, 453-460.

Hashin, Z. (1962) "The elastic Moduli of Heterogeneous Materials," *J. of Applied Mechanics,* Transaction of the ASME, March, 143-150.

Hobbs, D.W. (1988) Alkali-Silica Reaction in Concrete, Thomas Telford, London.

Jin, W. (1998) "Alkali-Silica Reaction in Concrete with Glass Aggregate - A Chemo-Physico-Mechanical Approach", Ph.D. Dissertation, Columbia University, New York.

Jin, W., Suwito, A., Meyer, C., and Xi, Y. (1998) "Theoretical Modeling on Expansion and Damage due to Alkali-Silica Reaction", Proceedings of 12th Engineering Mechanics Conference: *Engineering Mechanics: A Force for the 21st Century*, May 18-20, San Diego, CA., 1175-1178.

Johansen, V., Thaulow, N., and Skalny, J. (1993) "Simultaneous Presence of Alkali-Silica Gel and Ettringite in Concrete", *Advances in Cement Research*, 5(17), 23-29.

Meyer, C., and Xi, Y. (1999) "Use of Recycled Glass and Fly Ash for Precast Concrete", *Journal of Materials in Civil Engineering*, ASCE, May, 11(2), 89-90.

Meyer, C., and Baxter, S. (1998) "Use of Recycled Glass and Fly Ash for Precast Concrete", *Report NYSERDA 98-18 (9492-IABR-IA-96)* to New York State Energy Research and Development Authority, Dept. of Civil Engin. and Engin. Mechanics, Columbia University, New York.

Ping, X, Beaudon, J.J. and Brousseau, R., (1991) "Flat Aggregate Portland Cement Paste Interpaste", Cement and Concrete Research, 21, 718-726.

Prezzi, M., Monteiro, P.J.M., and Sposito, G. (1997) "The Alkali-Silica Reaction, Part I: Use Double-Layer Theory to Explain the Behavior of Reaction -Product Gels", *ACI Materials Journal*, 10-17.

Svensson, S.E. (1991) "Eigenstresses Generated by Diffusion in a Spherical Particle Embedded in an Elastic Medium", *Int. J. Mech. Sci.* 33(3), 211-223.

Ulm, F.J. Coussy, O., Kefei, L., and Larive, C. (2000) "Thermo-Chemo-Mechanics of ASR Expansion in Concrete Structures", *Journal of Engineering Mechanics*, ASCE, 126(3), 233-242.

Xi, Y., Suwito, A., Wen, X., Meyer, C., and Jin, W. (1999) "Testing and Modeling Alkali-Silica Reaction and the Associated Expansion of Concrete", *Mechanics of Quasi-Brittle Materials and Structures: A Volume in Honor of Prof. Z.P. Bazant's 60th Birth Day*, G. Pijaudier-Cabot, Z. Bittnar, B. Gerard (Editors), Hermes Science Publications, Paris, 217-232.

Xi, Y., and Bazant, Z.P. (1999) "Modeling Chloride Penetration in Saturated Concrete", *Journal of Materials in Civil Engineering*, ASCE, 11(1), 58-65

Xi, Y., and Jennings, H.M. (1997) "Shrinkage of Cement Paste and Concrete Modelled by a Multiscale Effective Homogeneous Theory", *Materials and Structures (RILEM*), 30, July, 329-339.

Xi, Y., Bazant, Z.P., and Jennings, H.M. (1995a) "Moisture Diffusion in Cementitious Materials: Adsorption Isotherm", *Journal of Advanced Cement-Based Materials*, 1, 248-257.

Xi, Y., Bazant, Z.P., and Jennings, H.M. (1995b) "Moisture Diffusion in Cementitious Materials: Moisture Capacity and Diffusivity", *Journal of Advanced Cement-Based Materials*, 1, 258-266.

Tabel 1. US Standard Sieve Series

ASTM	Specified sieve opening	
Sieve number	Micrometer	Inch
4	4760	0.187
8	2360	0.0937
16	1180	0.0469
30	600	0.0232
50	300	0.0117
100	150	0.0059
200	75	0.0029
325	45	0.0017
400	38	0.0015

Table 2. Material Parameters Used in the Analysis

Parameter	**Value**
Max. Time (days)	14
Volume Fraction of Aggregate	0.65
Volume Fraction of Matrix	0.35
κ_{ion}	1×10^{-10}
κ_{gel}	1.0×10^{-10}
Critical ion concentration, C_{crt}	0.005
Constant ion concentration, C_0	0.1
Volume ratio, η	1.75
Elastic modulus of matrix at age 28 days, $E_m(28)$ (GPa)*	12
Elastic modulus of aggregate, E_a (GPa)	80
V_{unit} (mm^3/mm^2)	0.002
Porosity, C_p (%)	40
Tensile strength of concrete, $f_t^{'}$ (MPa)	3
Poisson's ratio of matrix and aggregate	0.2

*$E_m(t) = \sqrt{\frac{t}{4+0.85t}}$

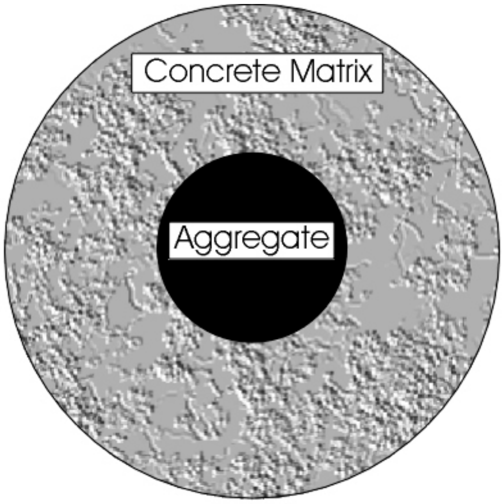

Fig. 1 Basic volume element

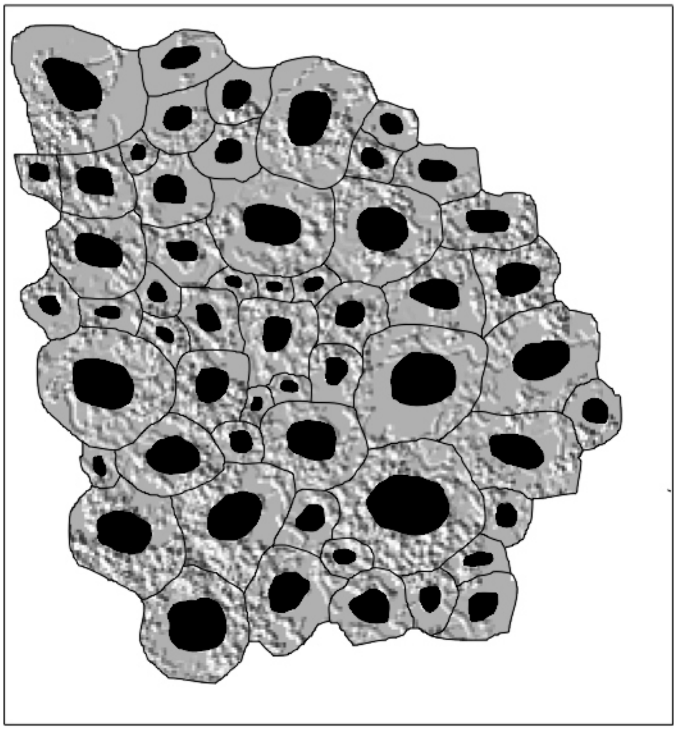

Fig. 2 Partition of basic element

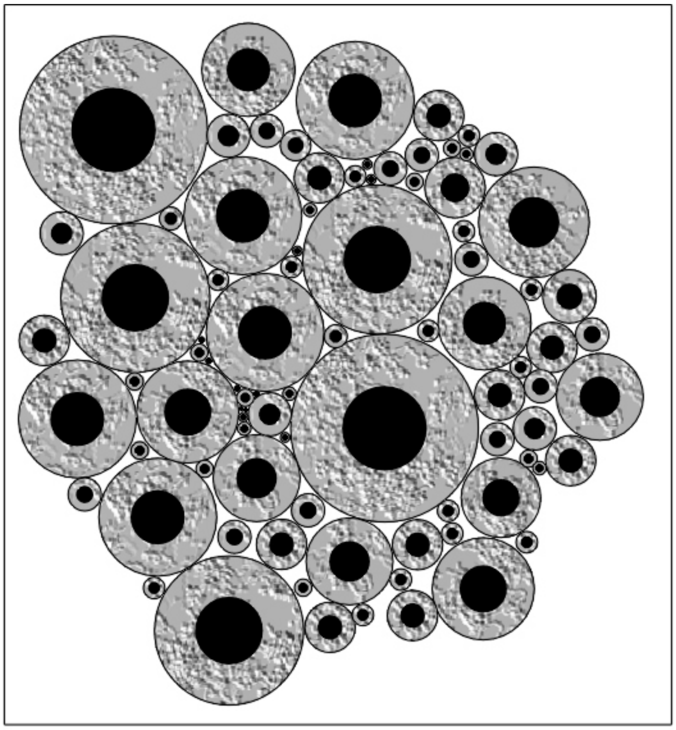

Fig. 3 Particle size distribution

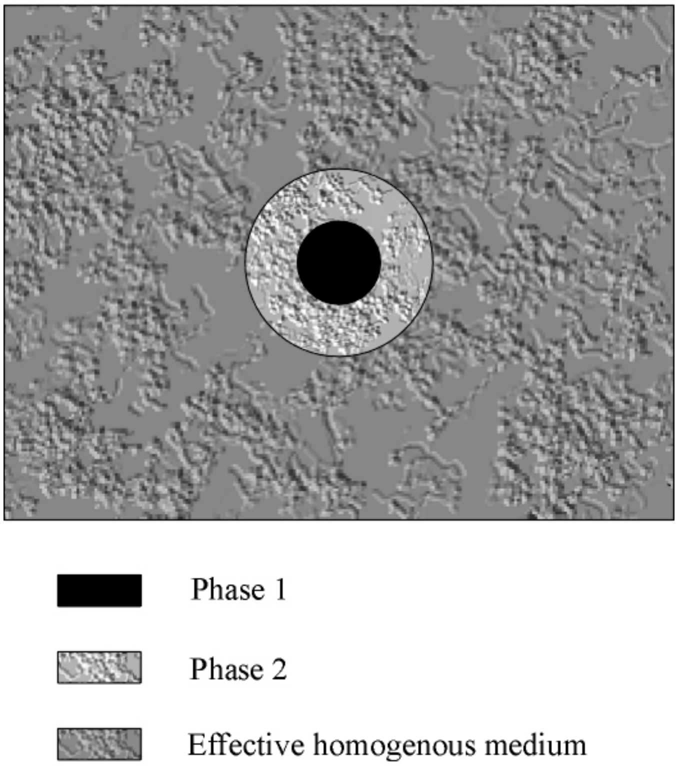

Fig. 4 Three phase model

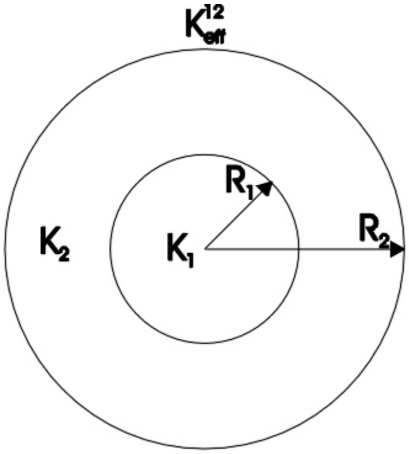

Fig. 5 Three phase expansion model

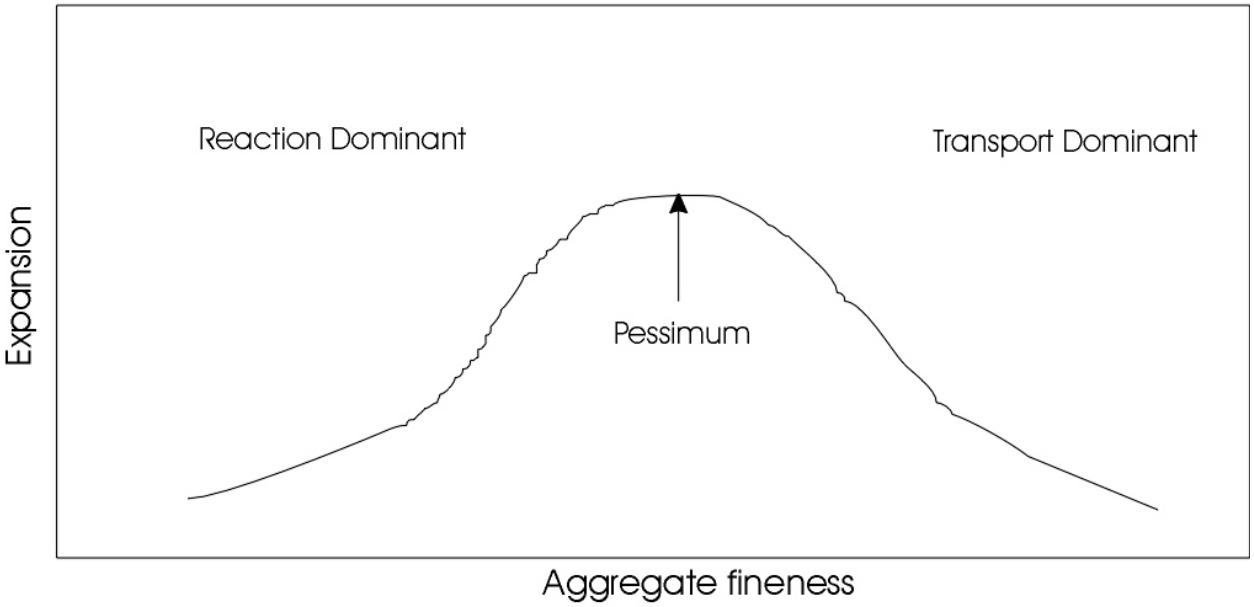

Fig. 6 Pessimum size effects as a results of two opposing processes

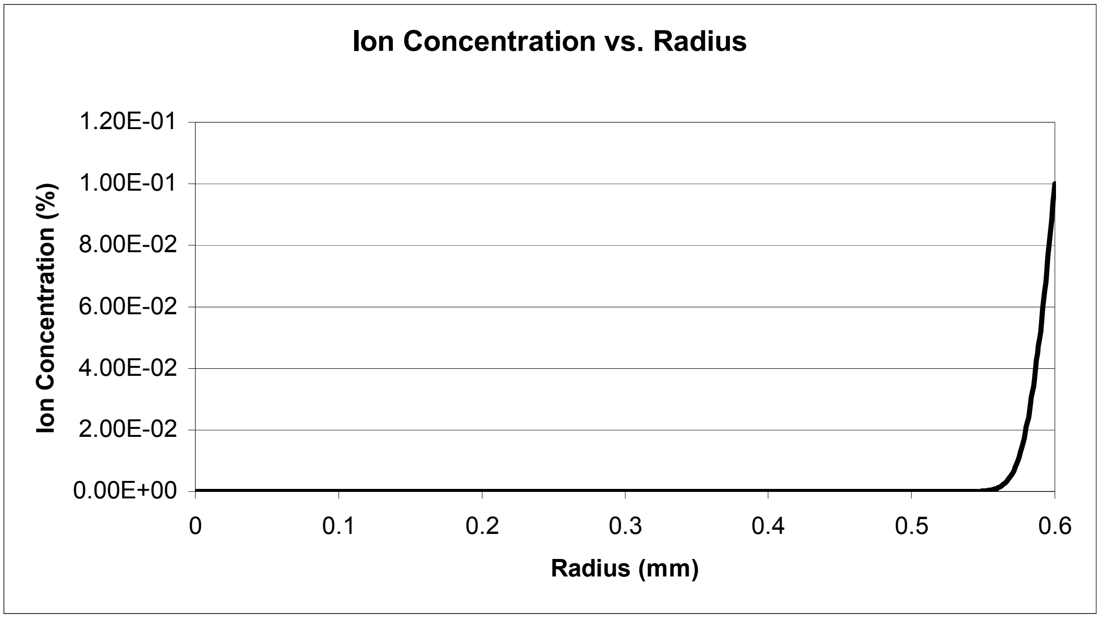

Figure 7. The Profile of ion concentration in the aggregate

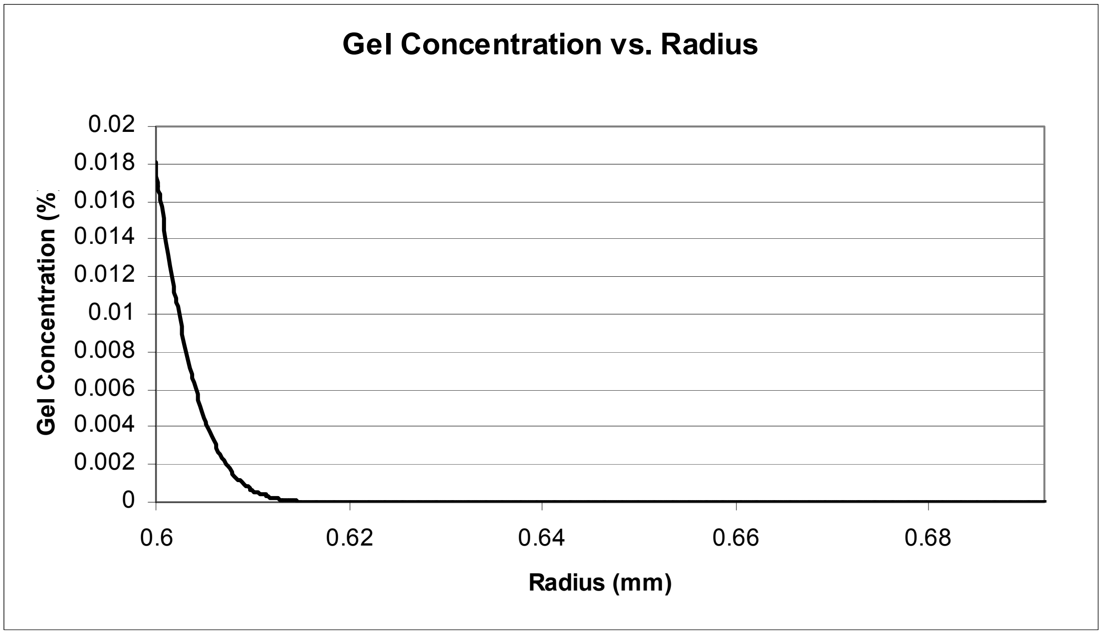

Figure 8. The profile of gel distribution in concrete matrix

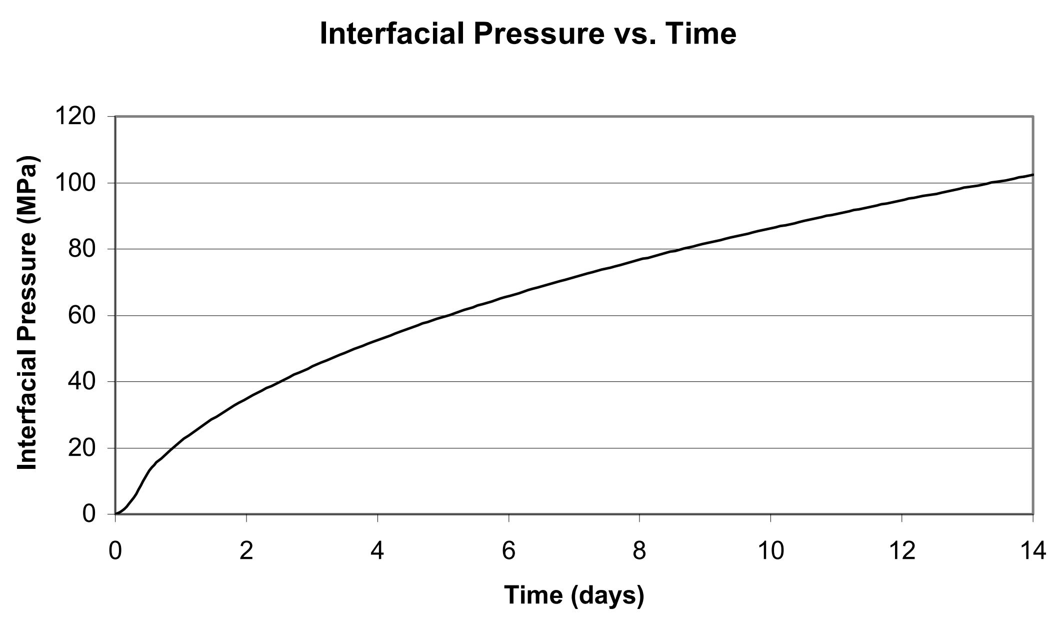

Figure 9. The development of the interface pressure with time

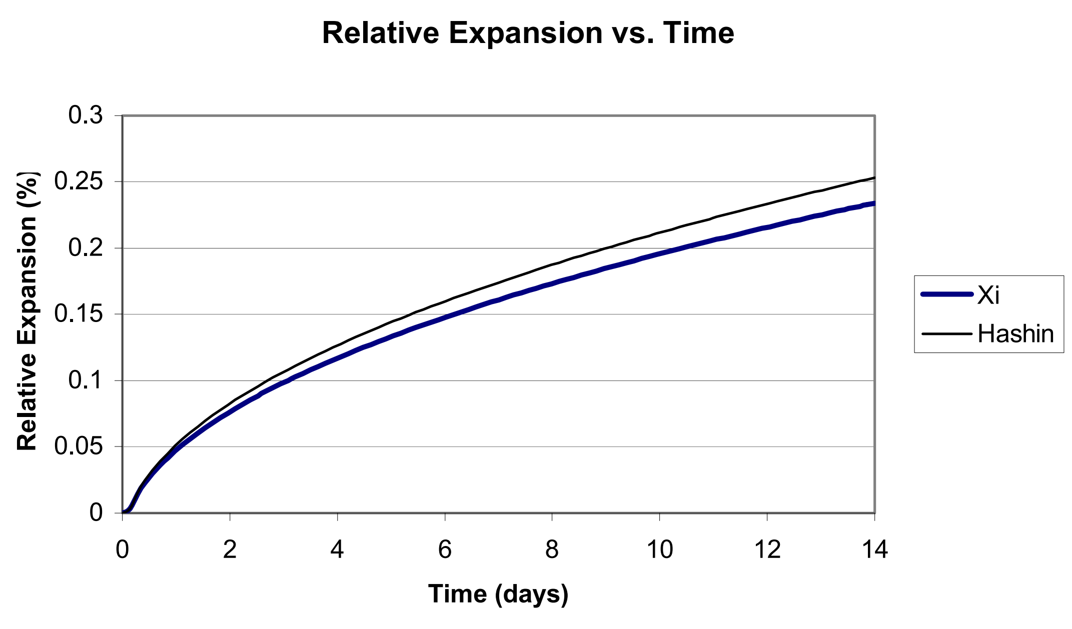

Figure 10. The increase of ASR expansion with time

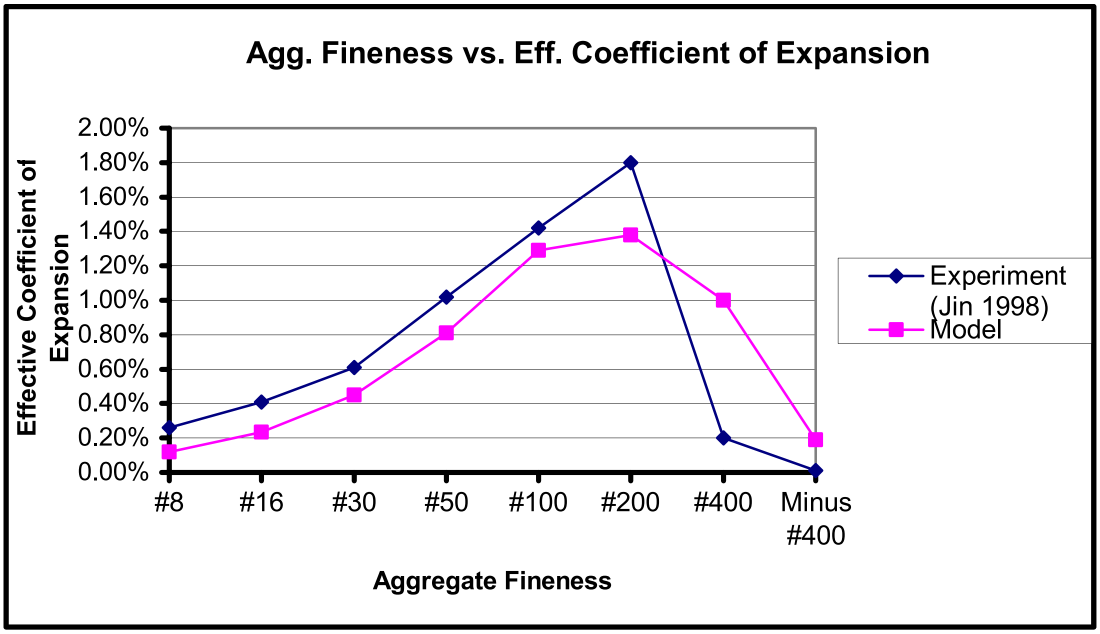

Figure 11. Expansion vs. Aggregate fineness